Renormalization approach to quantum-dot structures under strong alternating fields

P. A. Schulz
Instituto de Física "Gleb Wataghin," Universidade Estadual de Campinas, 13083–970 Campinas, São Paulo, Brazil

P. H. Rivera* and Nelson Studart
Departamento de Física, Universidade Federal de São Carlos, 13565–905 São Carlos, São Paulo, Brazil
(Received 4 October 2001; revised manuscript received 25 March 2002; published 8 November 2002)

We develop a renormalization method for the quasienergy spectra of low-dimensional structured systems under intense ac fields. These systems are emulated by tight-binding lattice models with a clear continuum limit of the effective-mass and single-particle approximations. The coupling to the ac field is treated nonperturbatively by means of the Floquet Hamiltonian. The renormalization approach gives an intuitive view of the electronic dressed states. The numerical advantage over a direct diagonalization of the Floquet Hamiltonian makes the method suitable for the study of dressed states of nanoscopic systems with realistic geometries, irrespective of the ac field intensity. Two numerical examples are discussed: a quantum dot, emphasizing the analysis of the effective-mass limit for lattice models and double-dot structures, for which we discuss the limit of the two-level approximation currently used in the literature.

DOI: 10.1103/PhysRevB.66.195310 PACS number(s): 73.21.La, 72.20.Ht

I. INTRODUCTION

The renormalization method, as a tool for studying the electronic structure of solids, has attracted attention some 20 years ago with the application to disordered low-dimensional systems.[1,2] More recently, the particular suitability of the method for studying strongly anisotropic solids started to deserve growing interest, such as in applications to semiconductor superlattices and conducting polymers.[3]

The aim of the present work is to apply the renormalization method to a different problem with the same formal structure: the dressed electronic spectra of semiconductor microstructures under intense ac fields.

Recent advances in semiconductor technology opened possibilities to design systems that are in the quantum limit in all spatial directions, establishing an important branch of what is nowadays called nanoscience. A double quantum dot, sometimes also called artificial molecule,[4] is an example of such systems and has been the object of intensive research from both theoretical[5–21] and experimental[22–32] points of view in the last few years. In particular, the response of quantum dots and double quantum dots to microwave fields has attracted renewed attention[33,34] and is directly concerned to our work.

Semiconductor microstructures can be described by lattice models, treated in a tight-binding framework, emulating the continuum limit of the effective-mass approximation.[35] Lattice models have been widely used in the context of disorder effects on electronic and transport properties of two-dimensional systems.[36] On the other hand, lattice models show a quite long history as a simulation tool of nanoelectronic devices, as well as quantum billiards and arrays of quantum dots and antidots in the presence of a magnetic field.[37]

The coupling to an ac field is nonperturbatively included using the Floquet method, by means of a procedure introduced by Shirley.[38] The Floquet method is widely used for the nonperturbative study of the interaction of atomic, molecular, and semiconductor nanostructures systems with a strong ac electric field. The time-independent infinite matrix Hamiltonian, obtained after the application of the Floquet-Fourier transformation over the time-dependent Schrödinger equation, describes entirely these processes without any further *ad hoc* hypothesis.

Hence, the effect of an intense ac field on the electronic spectra of a nanostructure, such as a quantum dot, is well described by an infinite Floquet matrix. However, due to the large vector basis necessary to describe the system in a tight-binding approximation for the lattice model, the eigenvalue calculations are practically impossible to be performed beyond a perturbative field intensity range. Indeed, intense ac field effects have been usually investigated for heuristic chain models for minibands in superlattices. Having such limitations in mind, we observe that the infinite Hamiltonian matrix has the structure of a simple tight-binding linear chain tridiagonal matrix—where the diagonal ''energy sites'' are now replaced by block matrices—that corresponds to the bare Hamiltonian of the system with or without an associated multiple of the photon energy, what will be called ''photon replicas.'' The off-diagonal elements, i.e., the ''hopping parameters'' are replaced by block matrices that describe the coupling of the system with the ac field.

These relationships allow us to develop an interesting and promising approach: the renormalization procedure, whereby the actual dimension of the system to be calculated is reduced to that of the lattice model for the bare system. Furthermore, since the quantity calculated is the density of states, one gets a step further than by direct diagonalization of the Floquet Hamiltonian, which provides only the quasienergy spectra without the spectral modulation as a function of the field intensity, as well as the strength hierarchy of these quasienergy spectra related to different photon replicas, as will be discussed.

The paper has the following structure. A brief introduction to the Floquet Hamiltonian is given at the beginning, followed by a comprehensive description of the renormalization method applied to the system. Afterwards examples of the numerical calculations are shown and discussed. We initially

focus on the validity of a lattice model for a quantum dot in the presence of intense ac fields. The second part of the results and discussion section will be centered on the ac field dependence on the bonding and antibonding states of an artificial molecule, i.e., a double-quantum-dot structure.

II. THEORY

A. The Floquet Hamiltonian

The energy spectrum of a bare electronic system will be described here by a tight-binding square lattice of *s*-like orbitals, considering only nearest-neighbor interaction. An ac field will be considered parallel to one of the square sides. Hence, the model for the bare electronic system coupled to an arbitrarily intense ac field is described by the Hamiltonian $H=H_o+H_{int}$, where

$$H_o=\sum_{l_1,l_2}\epsilon_{l_1,l_2}\sigma_{l_1,l_2}\sigma^{\dagger}_{l_1,l_2}+\frac{V}{2}\sum_{l_1,l_2}[\sigma_{l_1,l_2}\sigma^{\dagger}_{l_1+1,l_2}+\sigma_{l_1+1,l_2}\sigma^{\dagger}_{l_1,l_2}+\sigma_{l_1,l_2}\sigma^{\dagger}_{l_1,l_2+1}+\sigma_{l_1,l_2+1}\sigma^{\dagger}_{l_1,l_2}] \tag{1}$$

and

$$H_{int}=eaF\cos\omega t\sum_{l_1,l_2}\sigma_{l_1,l_2}l_1\sigma^{\dagger}_{l_1,l_2}. \tag{2}$$

Here $\sigma_{l_1,l_2}=|l_1,l_2\rangle$, $\sigma^{\dagger}_{l_1,l_2}=\langle l_1,l_2|$, where (l_1,l_2) are the (x,y) coordinates of the sites. The *atomic energy* will be taken constant, $\epsilon_{l_1,l_2}=4|V|$, for all sites. Equation (2) represents the coupling to the ac electric field parallel to the x axis, as can be seen by the linear dependence on l_1: e is the electron charge; ω and F are the monochromatic ac field frequency and amplitude, respectively. In the results shown throughout this work, the field direction will be parallel to one of the sides of an isolated quantum dot or along the double-quantum-dot structure. The treatment of the time-dependent problem is based on Floquet states $|l_1,l_2,m\rangle$ where m is the photon index. We follow the procedure developed by Shirley[38] for a two-level problem, which consists in a Fourier-Floquet transformation of the time-dependent Hamiltonian into a time-independent infinite matrix. The elements of this infinite matrix are

$$\left[(\mathcal{E}-m\hbar\omega-\epsilon_{l_1,l_2})\delta_{l_1'l_1}\delta_{l_2'l_2}-\frac{V}{2}\{(\delta_{l_1',l_1-1}+\delta_{l_1',l_1+1})\delta_{l_2'l_2}+(\delta_{l_2',l_2-1}+\delta_{l_2',l_2+1})\delta_{l_1'l_1}\}\right]\delta_{m'm}=F_1 l_1\delta_{l_1'l_1}\delta_{l_2'l_2}(\delta_{m',m-1}+\delta_{m',m+1}), \tag{3}$$

where $F_1=\frac{1}{2}eaF$. These matrix elements are similar to those reported in a long list of one-dimensional systems under intense ac fields. One can easily identify that the left-hand side of Eq. (3) represents a barelike electronic system. The difference is that the energy eigenvalues, $\mathcal{E}-m\hbar\omega$ are now quasienergies of a system dressed by photons shifted by multiples of the photon energy, usually called the mth photon replica of the system. The effect of the ac field is to couple different photon replicas as may be seen in the right-hand side of Eq. (3). The problem can only be handled by means of direct diagonalization, if the Floquet matrix is truncated to a reasonable dimension. This dimension is given by $L_1\times L_2(2M+1)$, where L_1 and L_2 are the number of atomic sites in each direction, while M is the maximum photon index. The resulting quasienergy spectrum (for the infinite system) is periodic defining quasi-Brillouin zones (QBZ), with the first QBZ spanning the range $-\hbar\omega/2\leqslant\mathcal{E}\leqslant\hbar\omega/2$. The number M, which determines how many photon replicas are taken into account, is chosen in order to satisfy a convergence condition: symmetric spectra relative to the QBZ edges for the few relevant replicas around $m=0$. Since the ac field couples a Floquet state defined by m photons to states with $m-1$ or $m+1$ photons, multiple photon processes become relevant with increasing field intensity, but it can also be seen that the coupling matrix elements are linearly dependent on the dimension of the system in the direction of the field polarization, as can be seen in the right-hand side of Eq. (3). Therefore, the direct diagonalization of the Floquet Hamiltonian becomes difficult for nonperturbative field intensities and large systems.

A truncated Floquet matrix is a tridiagonal block matrix given by

$$\mathsf{M}_F=\begin{pmatrix}\mathsf{E}^M & \mathsf{F} & & & & & & & \\ \mathsf{F} & \mathsf{E}^{M-1} & \mathsf{F} & & & & & & \\ & & \ddots & & & & & & \\ & & \mathsf{F} & \mathsf{E}^1 & \mathsf{F} & & & & \\ & & & \mathsf{F} & \mathsf{E}^0 & \mathsf{F} & & & \\ & & & & \mathsf{F} & \mathsf{E}^{-1} & \mathsf{F} & & \\ & & & & & \ddots & & & \\ & & & & & & \mathsf{F} & \mathsf{E}^{-M+1} & \mathsf{F} \\ & & & & & & & \mathsf{F} & \mathsf{E}^{-M}\end{pmatrix} \tag{4}$$

where $\mathsf{E}^M=(\mathcal{E}-m\hbar\omega)\mathsf{I}+\mathsf{H}_0$ is a $L_1\times L_2$ block matrix representing a photon replica with the matrix elements given by the left-hand side of Eq. (3). The coupling of the system with the intense ac electric field is represented by the off-diagonal blocks F, which are diagonal block matrices, with the elements given by

$$\mathcal{F}=F_1 l_1 \delta_{l_1' l_1}\delta_{l_2' l_2}. \tag{5}$$

The diagonalization of the problem is simply given by

$$\mathsf{M}_F=0. \tag{6}$$

The dimension of the problem can be reduced to $L_1\times L_2$ by means of a renormalization procedure. The first step is to define the associated Green's function[39] G,

$$\mathsf{M}_F\mathsf{G}=\mathsf{I} \tag{7}$$

This function will be projected onto the photon subspace and for the sake of clarity we will drop the site indices in the Floquet states: $|l_1,l_2,m\rangle\rightarrow|m\rangle$.

Since the Floquet states form a complete basis, $\Sigma|k\rangle\langle k|=1$, the Green's functions are given by

$$\sum_k \langle n|\mathsf{M}_F|k\rangle G_{km}=\delta_{nm}. \tag{8}$$

Having Eq. (4) in mind, the matrices $\langle n|\mathsf{M}_F|k\rangle$ are simply written as

$$\langle n|\mathsf{M}_F|n\rangle=\mathsf{E}^N \tag{9}$$

for $n=k$, where the quasienergies are redefined as $\mathcal{E}\rightarrow\mathcal{E}+i\eta$, with $\eta\rightarrow 0$; and

$$\langle n|\mathsf{M}_F|k\rangle=\mathsf{F} \tag{10}$$

if $n\neq k$.

B. Renormalization method

The quasidensity of dressed states of a system with $L_1\times L_2$ sites is obtained by successive ''renormalizations'' of the Floquet matrix M_F, using the expansion in Green's functions. The infinite set of Green's function, Eq. (8), is depicted below around the photon replica for $M=0$,

$$\begin{aligned}
&\vdots\\
\mathsf{E}^{-2}G_{-2,0} &= \mathsf{F}(G_{-3,0}+G_{-1,0}),\\
\mathsf{E}^{-1}G_{-1,0} &= \mathsf{F}(G_{-2,0}+G_{0,0}),\\
\mathsf{E}^{0}G_{0,0} &= \mathsf{I}+\mathsf{F}(G_{-1,0}+G_{1,0}),\\
\mathsf{E}^{1}G_{1,0} &= \mathsf{F}(G_{0,0}+G_{2,0}),\\
\mathsf{E}^{2}G_{2,0} &= \mathsf{F}(G_{1,0}+G_{3,0}),\\
&\vdots
\end{aligned} \tag{11}$$

where the dots represent the remaining equations of the infinite set. The decimation procedure consists in eliminating, from the above set of equations, all those equations involving odd-numbered photon replicas, i.e., by replacing the expressions

$$G_{2n+1,0}=\frac{1}{\mathsf{E}^{2n+1}}\mathsf{F}(G_{2n,0}+G_{2n+2,0}) \tag{12}$$

in the right-hand side of the subset for the even-numbered photon replicas $G_{2n,0}$ in Eq. (11). The result is a set of Green's functions with renormalized photon replicas and coupling matrices. This decimation procedure is successively applied to the remaining equations of the original set given in Eq. (11). The general form of these equations, after $\xi\geqslant 1$ decimations is

$$\mathsf{E}_\xi^M G_{m,0}=\delta_{m,0}+\mathsf{F}^\xi_{m-2^\xi,m}G_{m-2^\xi,0}+\mathsf{F}^\xi_{m+2^\xi,m}G_{m+2^\xi,0}, \tag{13}$$

where the renormalized photon replicas, up to order of ξ, are given by

$$\begin{aligned}
\mathsf{E}_\xi^M=\mathsf{E}_{\xi-1}^M &- \mathsf{F}^{\xi-1}_{m-2^{\xi-1},m}\frac{1}{\mathsf{E}^{m-2^{\xi-1}}_{\xi-1}}\mathsf{F}^{\xi-1}_{m,m-2^{\xi-1}}\\
&- \mathsf{F}^{\xi-1}_{m+2^{\xi-1},m}\frac{1}{\mathsf{E}^{M+2^{\xi-1}}_{\xi-1}}\mathsf{F}^{\xi-1}_{m,m+2^{\xi-1}}
\end{aligned} \tag{14}$$

while the coupling matrices, up to the same decimation order of ξ, are written as

$$\mathsf{F}^\xi_{m-2^\xi,m}=\mathsf{F}^{\xi-1}_{m-2^{\xi-1},m}\frac{1}{\mathsf{E}^{M-2^{\xi-1}}_{\xi-1}}\mathsf{F}^{\xi-1}_{m-2^\xi,m-2^{\xi-1}} \tag{15}$$

and

$$\mathsf{F}^\xi_{m+2^\xi,m}=\mathsf{F}^{\xi-1}_{m+2^{\xi-1},m}\frac{1}{\mathsf{E}^{M+2^{\xi-1}}_{\xi-1}}\mathsf{F}^{\xi-1}_{m+2^\xi,m+2^{\xi-1}}. \tag{16}$$

Although the successive decimation procedure described here is straightforward, we add a few comments for a clear understanding of the results shown in Eqs. (13)–(16). The coupling matrices, F, are all identical in the initial set of Green's-function equations, Eq. (8). Already after the first decimation, $\xi=1$, the coupling to higher and lower photon replicas become different, due to the addition or subtraction of $m\hbar\omega$ in the denominators, respectively. The expressions given by Eqs. (14)–(16) are actually recursive relations between renormalized quantities after ξ decimations and those from the previous step, i.e., $\xi-1$.

The renormalized expression for the photon replicas of the electronic system reveals a simple interpretation of the method: each decimation represents a successive dressing of the electronic states. By inspecting the coupling matrices, it is straightforward to realize that the coupling between photon replicas that are distant in energy by increasing multiples of $\hbar\omega$ becomes relevant only with increasing field intensity.

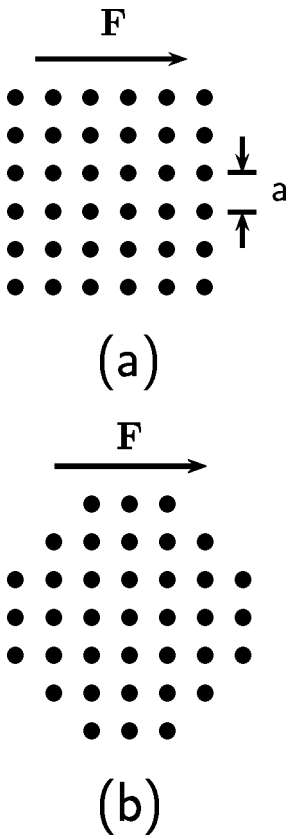

FIG. 1. Quantum-dot geometries (a) square, and (b) rounded square. The arrow indicates the ac-electric-field direction.

The final result of this renormalization of the Floquet matrix is the dressed Green's function for one of the photon replicas, such as $M=0$, with the proper renormalized photon replica and coupling matrices. This is achieved by substituting the results of Eqs. (14)–(16) into Eq. (13). The number of decimations necessary for a given field intensity is determined by a convergence criteria between a given step ξ with the previous one. A quasi-density-of-Floquet-states, $\rho(\mathcal{E}+i\eta)$ can then be obtained,

$$\rho(\mathcal{E}+i\eta)=-\frac{1}{\pi}\mathrm{Im}[\mathrm{Tr}\ \ G_{00}]. \tag{17}$$

The trace of the Green's operator is taken over the atomic sites basis. The present method can be seen as a version of the Floquet state theory in the Green's-function language, as discussed by Brandes.[40] Having in mind previous attempts,[33,40] the decimation procedure, besides the already mentioned intuitive interpretation for dressed states in such Green's-function language, has no limitations concerning the ac field strength and may be applied to arbitrary static potential profiles that define the bare mesoscopic systems.

C. Lattice and continuum limits

Lattice models, with nearest-neighbor interactions only, show a particle-hole symmetry in the electronic structure and are usually thought as simple, although useful, approximations for superlattices or arrays of quantum dots, where each quantum well or quantum dot is represented by a site of the lattice. This extreme lattice limit has been used throughout the literature for studying qualitatively the effect of intense ac fields on superlattice minibands, as already mentioned in the introduction. On the other hand, lattice models may be useful in emulating the lower part of electronic systems that are well described by the effective-mass approximation. In the present work, the tight-binding hopping parameter is chosen in order to emulate the electronic effective mass for the GaAs bottom of the conduction band, $m^*=0.067m_0$. Since, $V=-\hbar^2/(2m^*a^2)$, $V=-0.142$ eV for a lattice parameter of $a=20$ Å. Such parametrization used in the results shown below, will correspond to structures with lateral widths up to $L=280$ Å (double-quantum-dot case). This is still an order of magnitude lower than the typical dimensions of actual quantum dots constructed by lithographic methods. How-

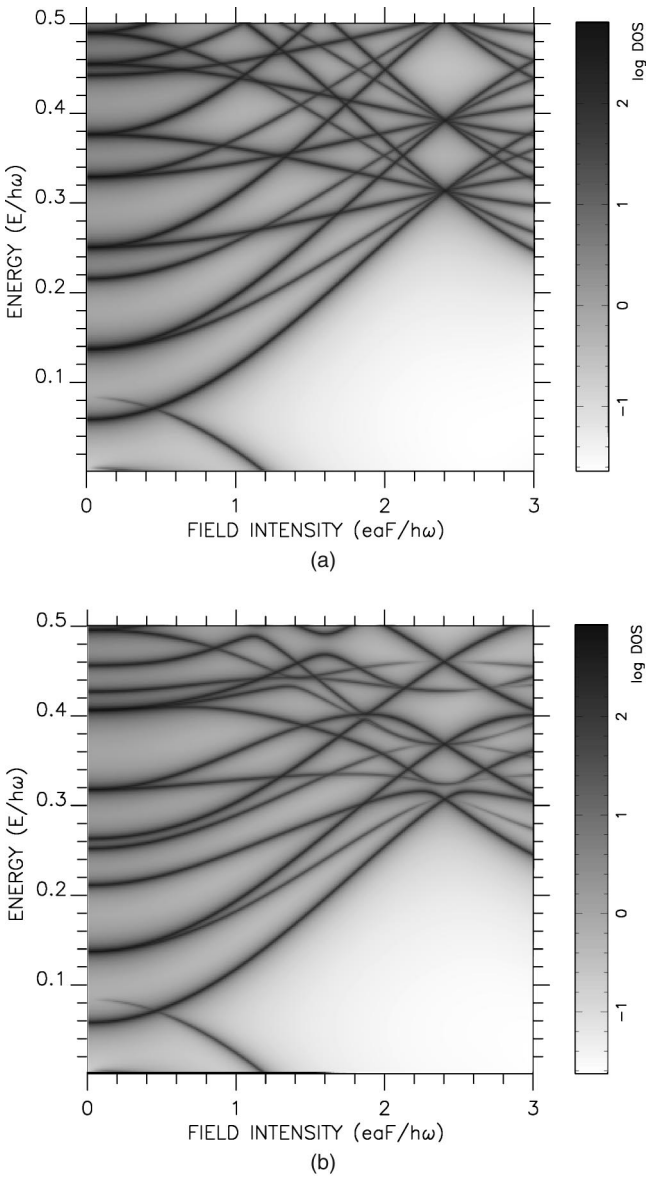

FIG. 2. Density of states as a function of field intensity, at a high frequency, $\hbar\omega=1$ eV, of a square lattice (top), and rounded lattice (bottom).

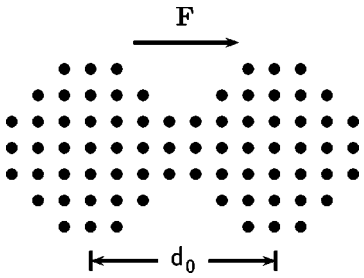

FIG. 3. Double-quantum-dot geometry. The arrow indicates the direction of the ac-electric-field considered.

ever, in the present study we intend to illustrate the method as well as to establish the range of validity of the lattice model for an effective-mass approximation physical limit. In this sense, the first question to be addressed is the transition between the extreme lattice and effective-mass limits. This is analyzed by following the evolution of the quasi-density-of-states as a function of the intensity-of-ac fields with frequencies of the order of the electronic bandwidth. Such an essential step has been carried out for rather small structures, as mentioned above. Once this point is settled, one can see that the general conclusions are consistent for larger quantum-dot systems. It should be also pointed out that we will be mainly concerned with the lowest pair of states of a double quantum dot. In such a situation, the atomic site basis is large enough to properly simulate these states.

III. ARTIFICIAL ATOMS AND MOLECULES

A. A quantum dot under intense ac field

As a starting point, we calculate the quasi-density-of-states of quantum dots as a function of the ac field intensity. We choose two different quantum-dot geometries: a square and a rounded one, as shown in Fig. 1, where the ac-electric-field direction is indicated by an arrow. The square quantum-dot is emulated by an array of 6×6 atomic sites, Fig. 1(b). A more realistic geometry for a quantum dot is given in Fig. 1(b), which will be used for the double-dot systems studied also in this work. It should be noticed that the area of this geometry—37 atomic sites, using the same tight-binding parameters described below—is comparable with the square one, Fig. 1(a). In Fig. 2 we show the contour plot of the density of states as a function of the ac field intensity for the bottom half of the first QBZ. We recall that, for the chosen hopping parameter, the bandwidth is given by $\Delta E=|8V|=1.136$ eV. Here the field frequency is $\hbar\omega=1.0$ eV. The square quantum dot, although a textbook example, is very useful to understand the breakdown of the effective-mass limit. At zero field intensity the energy spectrum of a two dimensional square potential well with $L=120$ Å—a quantum dot—is clearly identified, as well as the breakdown of degeneracies due to the applied ac field. The level shifts (ac Stark shift) lead to crossings at $eaF/\hbar\omega\approx2.4$, corresponding to a dynamic localization in chains perpendicular to the field direction. This is the limit where the host lattice effects are already predominant, i.e., the discrete basis of atomic orbitals does not emulate the effective-mass approximation

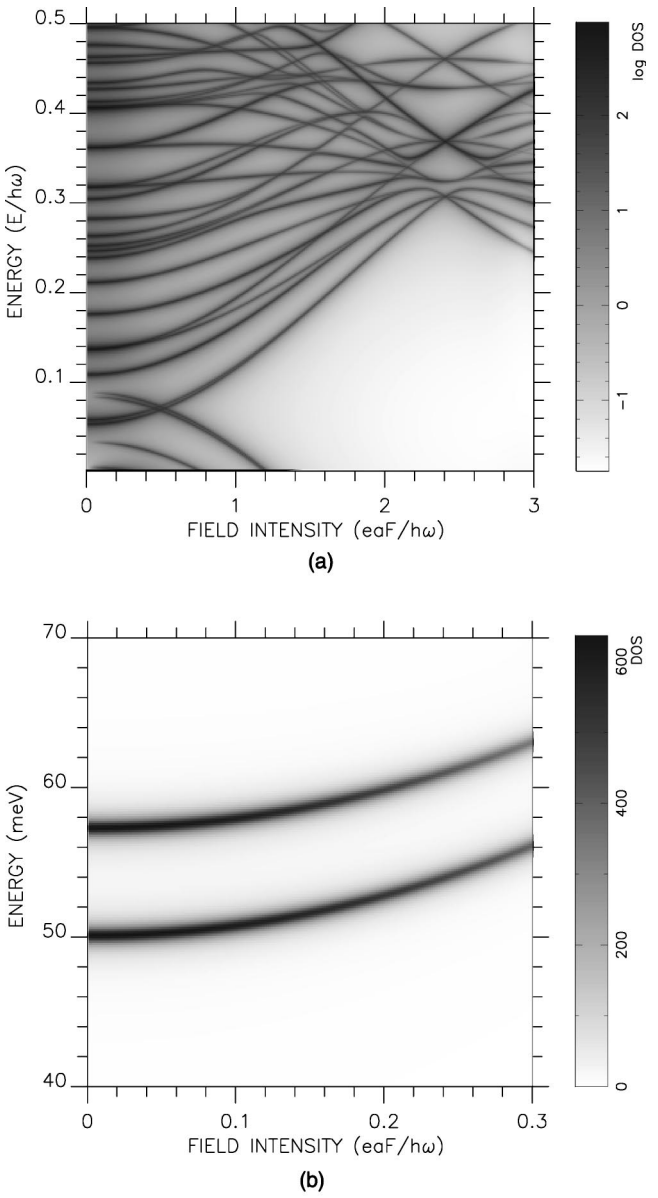

FIG. 4. Top: density of states as a function of field intensity of a double quantum dot, as shown in Fig. 3, at a high frequency, $\hbar\omega=1$ eV. Bottom: density of states for the two lowest states, i.e., the *molecular* bonding and antibonding states.

anymore and the length scale is given by the host lattice parameter a and not the lateral width, L, of the quantum dot. Indeed, the model simulates in this limit a square array of quantum dots, each one represented by a single site, resembling the results that would be expected for coupled chains, where each chain model the dynamic localization in superlattice minibands.

This result for a square array is a good guide for characterizing the density of states as a function of the field intensity of a quantum dot with lower symmetry, Fig. 1(b), as can be seen in the equivalent plot shown in Fig. 2(b) also for a frequency $\hbar\omega=1.0$ eV. The dynamic localization at the extreme lattice limit is less defined due to the fact that the atomic site chains perpendicular to the field direction are not

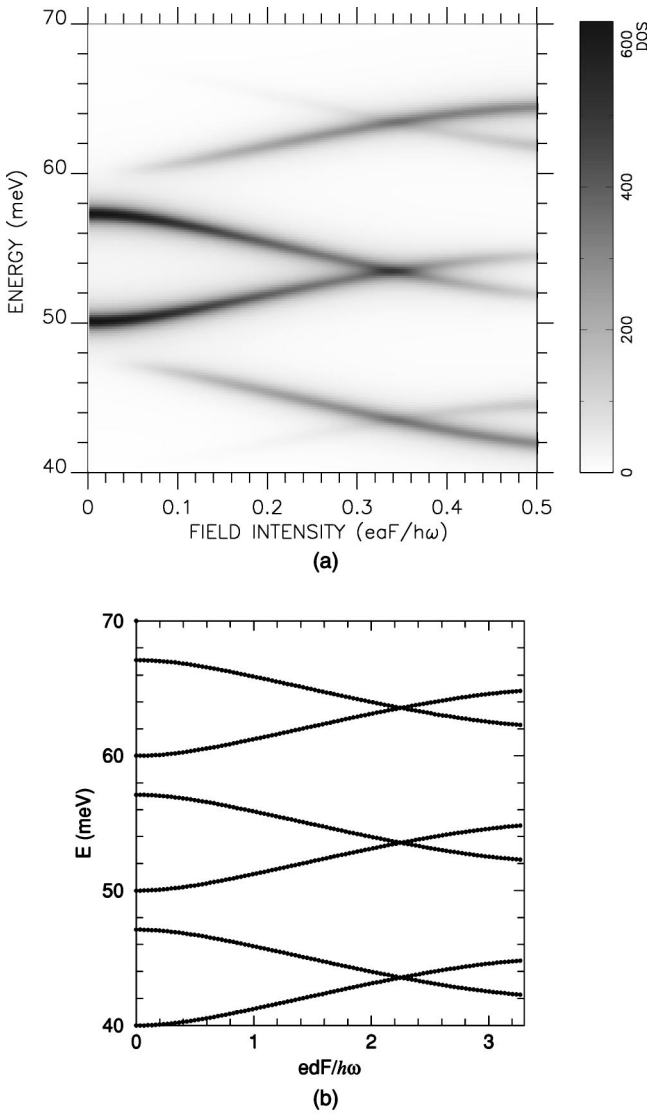

FIG. 5. Top: Density of states as a function of field intensity of a double quantum dot at low frequencies, $\hbar\omega = 10$ meV. Bottom: spectra of an equivalent two-level system, simulated with a dipole distance $d \approx d_0$, in the dynamic localization regime.

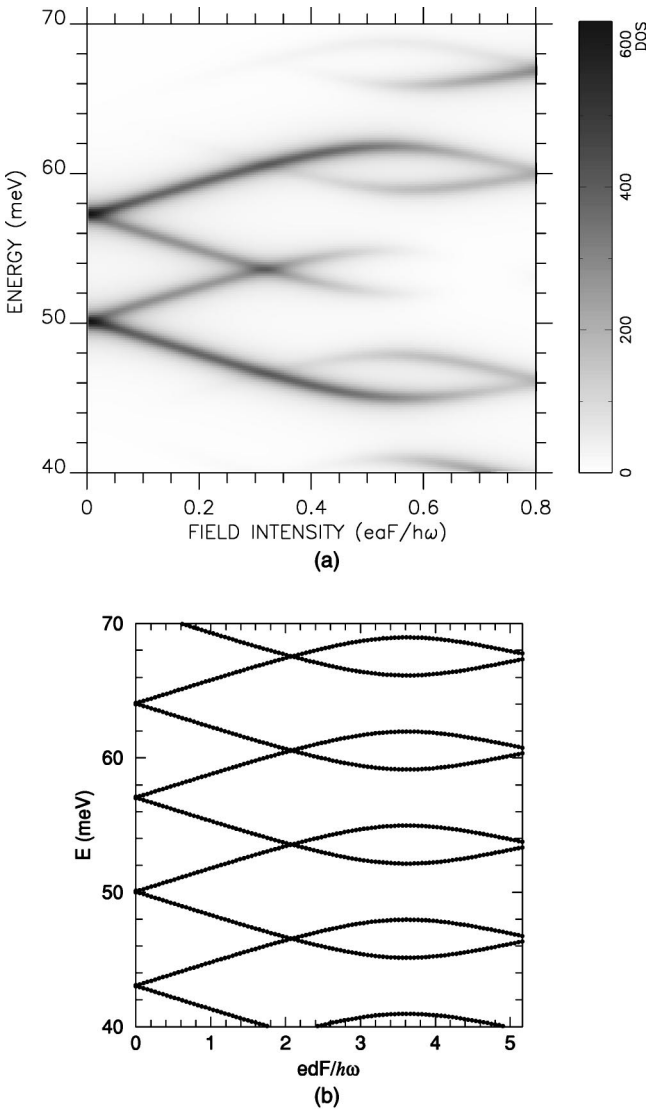

FIG. 6. Top: Density of states of a double quantum dot as a function of field intensity at a nearly resonant frequency, $\hbar\omega = 7$ meV. Bottom: spectra of a two-level equivalent system near Rabi resonance.

equivalent as in the square array. Besides that some of the degeneracies are already broken in the absence of the ac field.

A important characteristic of the method can be seen in Fig. 2. By simply diagonalizing the Floquet Hamiltonian, the quasienergy spectra are depicted in the so-called QBZ's, each of them reproducing the spectrum with the energy shifted by integer multiples of the photon energy. The overlap of these photon replicas makes the interpretation of the spectrum rather cumbersome, specially for strong overlaps, which are unavoidable for low frequencies. The result of the present renormalization approach is the quasienergy spectrum modulated by the field-dependent density of states, so the higher or lower photon replica become relevant only with increasing field intensity. This effect is verified at the bottom of Figs. 2(a) and 2(b): the spectrum replica lowered by one photon energy shows a negligible contribution at low-field intensity. On the other hand, in both figures we see no significant modulation of the density of states in the low-field intensity limit within the entire band of the depicted zero photon replica, due to the high frequency considered.

The main interest, however, is the effective-mass limit, i.e., the energy bottom of each photon replica at low-field intensities in the scale of Fig. 2, as well as low frequencies that would couple only these few low-energy states. The scaling of these quantities shows the suitability of the present method, as will be seen in the following discussion on double quantum dots.

B. Double Quantum dot

The double-quantum-dot system is based on the quantum dot shown in Fig. 1(b). The coupling between dots is of free choice and we consider a simple connection of both dots by

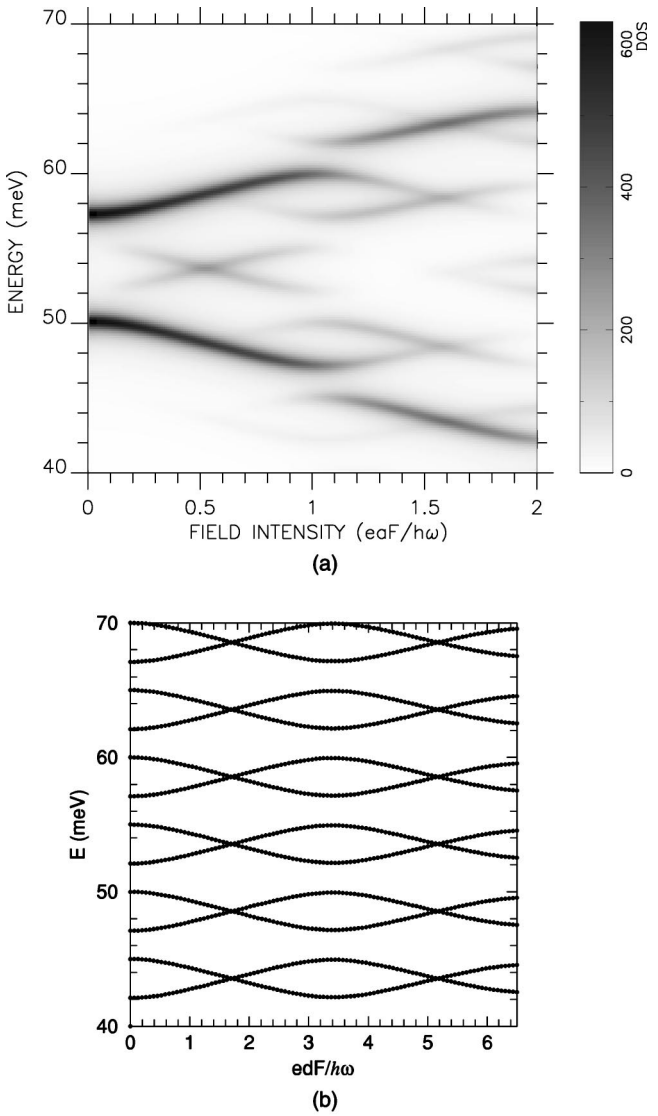

FIG. 7. Top: Density of states of a double quantum dot as a function of field intensity at $\hbar\omega=5$ meV. Bottom: spectra of a two-level system in the ac Stark regime.

the same hopping parameters considered so far, as illustrated in Fig. 3. Such configuration is an example of strong interdot coupling. As stated before, the ac field direction is along the quantum-dot *molecule*. The corresponding quasi-density-of-states plot as a function of field intensity for the same high-field frequency, $\hbar\omega=1.0$ eV, as in Fig. 2 is shown in Fig. 4(a). The quasi-density-of-states spectrum is very similar with the appearance of the expected energy splitting due to the coupling among quantum-dot states. The energy splitting structure may be rather complex, considering the coupling of initially degenerate states in each quantum dot. A covalent-like binding, with a splitting between bonding and antibonding states is well defined for the interdot coupling between the lowest state in each quantum dot. Therefore, from now on we will focus exclusively on the energy bottom of the spectra, the continuum—low-field intensity—limit, in order to analyze the lowest pair of split double-quantum-dot states.

In Fig. 4(b) we have the quasi-density-of-states for the lowest pair of molecular states. Both, bonding and antibonding states shift rigidly upwards in energy. Here a modulation of the density of states is seen: with the increasing field intensity, the density of states diminishes, with increasing contribution of higher and lower photon replicas (not shown). Since the frequency of the field is very high $\hbar\omega=1$ eV, all states of the system are mixed by the field and no typical two-level behavior is observed. The rigid energy shift may be seen already as a lattice effect, since for high-field intensities the dynamic localization for the host lattice is revealed, Fig. 4(a).

A clear covalent molecular picture is revealed for much lower frequencies, in the range of $\hbar\omega\approx 10$ meV, which is of the order of the tunnel splitting between the lowest pair of states in the bare ''molecule''" for the chosen parameters: $\Delta E_{split}=7.1$ meV. For this frequency range the coupling to higher molecular states is negligible, since the third molecular state is about 50 meV above the antibonding state. The lattice effects are also absent, since the dynamic localization effects on the host lattice are relevant for field frequencies of the order of the entire spectral width, which is two orders of magnitude larger than the energy scale of interest: the tunnel splitting. The present results are exact, since we are in an independent particle approximation for an artificial H_2^+ molecule. Within this parameter range, the lowest pair of states of the double quantum dot behave as a two-level system,[32] as will be discussed in the following results. We are going to switch the field frequency from above to below the tunnel splitting energy. The quasi-density-of-states plots will also be compared to the corresponding quasienergy spectra of the equivalent two-level system obtained by diagonalizing the Floquet Hamiltonian.

In Fig. 5 the evolution of the artificial $H_2{}^+$ bonding and antibonding states as functions of field intensity is shown for a field frequency $\hbar\omega=10$ meV$>\Delta E_{split}$. In Fig. 5(a) we see the quasi-density-of-states around the main photon replica, which shows the highest intensity for low-field intensities. The next important branches of the quasi-density-of-states are the bonding state plus one photon and the antibonding minus one photon. With increasing field intensity, the splitting between the zero-photon bonding and antibonding states diminishes down to a crossing at $eaF/\hbar\omega\approx 0.3$. This resembles the dynamic localization regime for superlattice minibands[41,42] The branches of the quasi-density-of-states in Fig. 5(a) can be mapped on the quasienergy spectrum of a two-level system, emulated by two atomic sites with fitted tight-binding parameters. This spectrum is a function of a field intensity defined by $edF/\hbar\omega$, where d is the distance between the two effective atomic sites. The correspondence between Figs. 5(a) and 5(b) is satisfied by properly scaling $d\approx 7a$. Having in mind the double quantum dot of Fig. 3, $d=7a$ is the distance between the centers of the dots,[41] ''the bond length of the molecule.''

A similar situation, for a field frequency given by $\hbar\omega=7$ meV, therefore near a resonance situation, $\Delta E_{split}\approx\hbar\omega$; is shown in Fig. 6. Here we clearly see that the bonding and antibonding states evolve in *Rabi sidebands*.[43] This behavior can also be mapped on an effective two-level sys-

tem, Fig. 6(b). The effective distance between the two effective atomic sites is close to the ''molecular bond length'' $d=7a$, as for frequencies higher than the tunnel splitting, Fig. 5.

The near resonant case may be analyzed directly from the Rabi frequency at the crossing of the sidebands in Fig. 6(a). At the crossing $\hbar\omega_R=\Delta E_{split}$, where $\omega_R=d_0F/\hbar$ with d_0 being the dipole matrix element. Since $\Delta E_{split}=\hbar\omega$, one has that $eaF\approx 0.3\hbar\omega_R$, resulting in a dipole matrix element $d_0\approx 3.33a$ and $2d_0=6.6a$, in good agreement with the ''molecular length,'' $d=7a$.

In Fig. 7 we show the situation for a field frequency $\hbar\omega=5$ meV lower than the bare tunneling splitting. The zero-photon molecular states show an ac Stark shift,[43] Fig. 7(a). The dressed tunnel splitting increases with field intensity up the first important anticrossing at $eaF/\hbar\omega=1$. Now the mapping on an effective two-level system, Fig. 7(b), occurs for an effective distance $d\approx 3.5$, nearly half the nominal molecular bond length. This shrinking of the effective distance is, however, compatible with the increasing of the tunnel splitting.

IV. FINAL REMARKS

In the present work we have developed a renormalization-decimation method applicable to the Floquet Hamiltonian. With this method it becomes possible to investigate intense ac field effects on semiconductor microstructures described by lattice models with realistic dimensions. The matrix dimension in the renormalization method is simply the number of lattice sites, $L_1\times L_2$, while for a direct diagonalization of the Floquet Hamiltonian one has to handle matrix dimensions of $L_1\times L_2(2M+1)$. The usefulness of the method can be illustrated with a simple estimate. In a previous work,[42] using a direct diagonalization procedure, strong field intensities required $M\approx 90$ for a chain $L\approx 20$ sites long. Therefore, in such cases the matrix dimension reaches $L(2M+1)=3620$, which is equivalent to the numerical effort of systems with lateral sizes of the order of $L_{1,2}\approx 60$ ($L_1\times L_2=3600$), using the renormalization-decimation method. Recalling the tight-binding parameters of the present work, this lateral size corresponds to $L=L_{(1,2)}a=1200$ Å, which is of the order of actual quantum dot typical length scales. The illustrative examples shown here for double quantum dots are still heuristic, since one of the main proposals of this work is the establishment of the continuum and extreme lattice limits of the model. This clear definition of the continuum limit permits the future application of the method to systems with dimensions at least one order of magnitude larger than the present heuristic ones. Nevertheless, the results for the rather small double quantum dots point out interesting dependences of the dressed electronic structure on the field frequency, which could be addressed in actual systems. A natural extension of the work is the analysis of the local quasi-density-of-states, as well as the study of asymmetric double quantum dots with realistic dimensions, a situation for which the density of states reveals actual tunneling properties.

ACKNOWLEDGMENTS

It is a pleasure to thank H. S. Brandi for suggesting the possibility of decimating the Floquet Hamiltonian, as well as many stimulating discussions at the beginning of this work. The authors acknowledge financial support from FAPESP and CNPq.

*Present address: Consejo Superior de Investigaciones, Universidad Nacional Mayor de San Marcos, Lima, Peru.

[1] H. Aoki, J. Phys. C **13**, 3369 (1980).
[2] C.E.T.G. da Silva and B. Koiller, Solid State Commun. **40**, 215 (1981).
[3] R. Farchioni, P. Vignolo, and G. Grosso, Phys. Rev. B **60**, 15705 (1999).
[4] L. Kouwenhoven, Science **268**, 1440 (1995).
[5] G.W. Bryant, Phys. Rev. B **44**, 3064 (1991).
[6] G. Klimeck, G. Chen, and S. Data, Phys. Rev. B **50**, 2316 (1994).
[7] C. Niu, L. Liu, and T. Lin, Phys. Rev. B **51**, 5130 (1995).
[8] J.J. Palacios and P. Hawrylak, Phys. Rev. B **51**, 1769 (1995).
[9] J.H. Oh, K.J. Chang, G. Ihm, and S.J. Lee, Phys. Rev. B **53**, R13264 (1996)
[10] R. Kotlyar and S.D. Sarma, Phys. Rev. B **55**, R10205 (1997).
[11] T. Aono and K. Kawamura, Jpn. J. Appl. Phys., Part 1 **36**, 3936 (1997).
[12] H. Aoki, Physica E (Amsterdam) **1**, 198 (1997).
[13] T. Pphjola, J.K.M.M. Salomaa, J. Schmid, H. Schoeller, and G. Schön, Europhys. Lett. **40**, 189 (1997).
[14] P. Brune, C. Bruder, and H. Schoeller, Phys. Rev. B **56**, 4730 (1997).
[15] O. Mayrock, S.A. Mikhailov, T. Darnhofer, and U. Rössler, Phys. Rev. B **56**, 15760 (1997).
[16] N.E. Kaputkina and Y.E. Lozovik, Phys. Solid State **40**, 1929 (1998).
[17] H. Imamura, H. Aoki, and P.A. Maksym, Phys. Rev. B **57**, R4257 (1998).
[18] Y. Asano, Phys. Rev. B **58**, 1414 (1998).
[19] W. Xie and C. Chen, Phys. Lett. A **245**, 297 (1998).
[20] C.A. Stafford, R. Kotlyar, and S.D. Sarma, Phys. Rev. B **58**, 7091 (1998).
[21] B. Partoens and F.M. Peeters, Physica B **298**, 282 (2001).
[22] A. Lorke and J.P. Kotthaus, Phys. Rev. Lett. **64**, 2559 (1990).
[23] M. Tewordt, R.J.F. Hughes, L.M. Moreno, J.T. Nichols, H. Asahi, M.J. Kelly, V.J. Law, D.A. Ritchie, J.E.F. Frost, G.A.C. Jones, and M. Pepper, Phys. Rev. B **49**, 8071 (1994).
[24] F.R. Waugh, M.J. Berry, D.J. Mar, R.M. Westerveit, K.L. Campman, and A.C. Gossard, Phys. Rev. Lett. **75**, 705 (1995).
[25] D. Dixon, L.P. Kouwenhoven, P.L. McEuen, Y. Nagamune, J. Motohisa, and H. Sakaki, Phys. Rev. B **53**, 12625 (1996).
[26] R.H. Blick, R.J. Haug, J. Weiss, D. Pfannkuche, K.v. Klitzing, and K. Eberl, Phys. Rev. B **53**, 7899 (1996).
[27] T. Schmidt, R.J. Haug, K.v. Klitzing, A. Förster, and H. Lüth, Phys. Rev. Lett. **78**, 1544 (1997).
[28] R.H. Blick, D.W. van der Weide, R.J. Haug, and K. Eberl, Phys. Rev. Lett. **81**, 689 (1998).
[29] R.H. Blick, D. Pfannkuche, R.J. Haug, K.v. Klitzing, and K.

Eberl, Phys. Rev. Lett. **80**, 4032 (1998).
[30] T.H. Oosterkamp, T. Fujisawa, W.G. van der Wiel, K. Ishibashi, R.V. Hijman, S. Tarucha, and L.P. Kouwenhoven, Nature (London) **395**, 873 (1998).
[31] T.H. Oosterkamp, S.F. Godijn, M.J. Uilenreef, Y.V. Nazarov, N.C. van der Vaart, and L.P. Kouwenhoven, Phys. Rev. Lett. **80**, 4591 (1998).
[32] T. Fujisawa, T.H. Oosterkamp, W.G. van der Wiel, B.W. Broer, R. Aguado, S. Tarucha, and L.P. Kouwenhoven, Science **282**, 932 (1998).
[33] Q.F. Sun, J. Wang, and T.M. Liu, Phys. Rev. B **61**, 12643 (2000).
[34] W.G. van der Wiel, T. Fujisawa, S. Tarucha, and L.P. Kouwenhoven, Jpn. J. Appl. Phys., Part 1 **40**, 2100 (2001).
[35] B. Huckestein, Rev. Mod. Phys. **67**, 357 (1995).
[36] See, for instance, E. Louis, and J.A. Verges, Phys. Rev. B **61**, 115310 (2001).
[37] See, for instance, I.V. Zozoulenko, F.A. Maao, and E.H. Hauge, Phys. Rev. B **51**, 7058 (1995).
[38] J.H. Shirley, Phys. Rev. **138**, B979 (1963).
[39] E.N. Economou, *Green's Functions in Quantum Physics* (Springer Verlag, Berlin, 1983).
[40] T. Brandes, Phys. Rev. B **56**, 1213 (1997).
[41] M. Holthaus, Z. Phys. B: Condens. Matter **89**, 251 (1992).
[42] P.H. Rivera and P.A. Schulz, Phys. Rev. B **61**, R7865 (2000).
[43] H. Haug and S.W. Koch, *Quantum Theory of the Optical and Electronic Properties of Semiconductors* (World Scientific, Singapore, 1990).